
Original Paper (Invited)

Experiment Investigation on Fluid Transportation Performance of Propellant Acquisition Vanes in Microgravity Environment

Baotang Zhuang¹, Yong Li¹, Xianwu Luo^{2*}, Halin Pan¹ and Jingjing Ji²

¹ Beijing Institute of Control Engineering, Beijing, 100190, China
zbt07@mails.tsinghua.edu.cn, ly00@mails.tsinghua.edu.cn

² Beijing Key Laboratory of CO₂ Utilization and Reduction Technology, Tsinghua University, Beijing 100084, China, luoxw@tsinghua.edu.cn, jijj12@mails.tsinghua.edu.cn

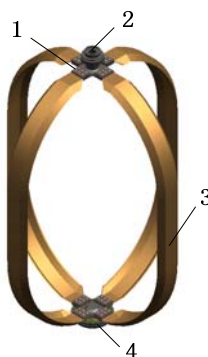
Abstract

The propellant acquisition vane (PAV) is a key part of a vane type surface tension propellant management device (PMD), which can manage the propellant effectively. In the present paper, the fluid transportation behaviors for five PAVs with different sections were investigated by using microgravity drop tower test. Further, numerical simulation for the propellant flow in a PMD under microgravity condition was also carried out based on VOF model, and showed the similar flow pattern for PAVs to the experiment. It is noted that the section geometry of PAVs is one of the main factors affecting the fluid transportation behavior of PMD. PAVs with bottom length ratio of 5/6 and 1/2 have larger propellant transportation velocity. Based on the experiments, there were two stages during the process of propellant transportation under microgravity environment: liquid relocation and steady transportation stage. It is also recognized that there is a linear correlation between liquid transportation velocity and relative time's square root. Those results can not only provide a guideline for optimization of new vane type PMDs, but also are helpful for fluid control applications in space environment.

Keywords: Microgravity, Propellant Acquisition Vanes, Fluid transportation, Experiment

1. Introduction

The vane type propellant management device (PMD) is frequently used to actively manage and control the liquid fuel in a propellant tank. For the PMD, it is the effect of surface tension that helps propellant acquisition vanes to realize gas-liquid separation, and liquid transportation^[1-4]. A vane type PMD is suitable for various kinds of propellant in different microgravity cases, especially for the large satellite platform with low-level microgravity. Figure 1 illustrates the typical structure of a PMD with 4 parallel vanes.



1. Blade adapter 2. Gas port 3. Parallel PAV
4. Bubble filter

Fig. 1 Typical structure of a vane type PMD

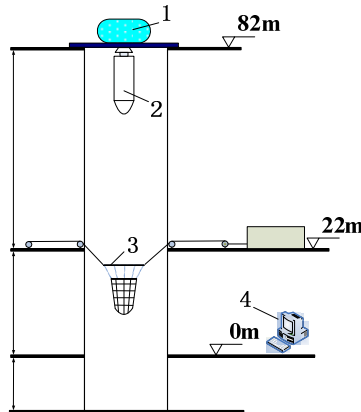
For a vane type PMD, the propellant acquisition vane (PAV) is a key part, which should continuously supply propellant without any gas. The characteristics of a PAV not only decide the propellant transportation ability, but also alleviate liquid sloshing effectively and improve the control precision of spacecraft.

Though much research on PMD with vane type have being carried out [5-12] since the early 1970s, further performance improvement of vane type PMD is necessary and important due to the emphasis on the operation stability of spacecrafts.

In present paper, the fluid transportation behaviors of propellant acquisition vanes with different sections were investigated by microgravity drop tower test. The effects of section geometry of PAVs were discussed based on experimental results and numerical analysis.

2. Test methods and PAV models

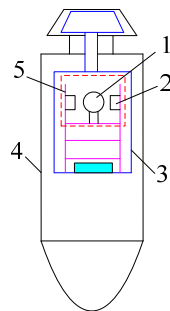
The propellant transportation performances of different PAVs were investigated experimentally using the microgravity (μg) drop tower at National Microgravity Laboratory, Chinese Academy of Science (NMLC) [13]. The test system can provide a gravitational acceleration near $10^{-5} g$ and keep the microgravity during 3.5 seconds. As shown in Figure 2, the facility includes a double-cabin, deceleration and recovery system, delivery system, control system, measurement system and other auxiliaries. The whole microgravity drop tower test system is illustrated.



1. Delivery system 2. Double-cabin 3. Deceleration and recovery system 4. Control system

Fig. 2 Sketch of μg drop tower test system

In order to reduce the air friction during the test process, the outer cabin of the double-cabin is designed as axisymmetrical shape as shown in Figure 3. In the inner cabin where the test load is installed, the pressure is less than 30Pa. During the test, the outer cabin falls free in atmosphere, and the inner cabin moves with the outer cabin together. Because the velocity difference between inner and outer cabin is negligible, the air friction acting on the inner cabin is very small. Thus, the gravitational acceleration in inner cabin can reach $10^{-5} g$ or less.



1. Test model 2. Image acquisition device 3. Inner cabin
4. Outer cabin 5. Test stand

Fig. 3 Illustration of a double-cabin.

In order to monitor the propellant transportation behavior of PAVs, a 4-channel CCD image device is adopted to take pictures with 25 frames per second.

Five PAVs with different sections shown in Figure 4 named as Model 1~5 are tested. It is seen that Model 5 has triangle section, Model 1 has rectangle section, and the other have trapezoid shapes. The width b_0 of each section is the same, and the total height for the PAVs i.e. h_0 is also constant. The bottom length ratios of those models i.e. $a_1/a_0, a_2/a_0, a_3/a_0, a_4/a_0, a_5/a_0$ are 1, 5/6, 1/2, 1/3, 0.

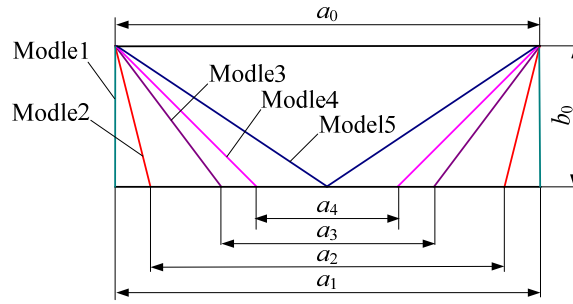


Fig. 4 PAV models with different sections

The PAVs and the reservoir for test fluid are made from plexiglass, whose refractive index is 1.491 and transmittance is 90%. The PAVs are fixed in a transparent test sump and the vane is set parallel to the surface of sump. The relative parallel distance to sump surface d/a_0 is 1/6. Initial relative height of the test fluid h_1/h_0 in the reservoir is 1/19. For convenience, two kinds of PAVs are fixed in the reservoir and tested at the same falling process. To prevent the disturbance between two PAVs, the distance between two vanes, and that between vanes and the inner surface of reservoir are large enough.

Absolute alcohol, whose physical properties are list in Table 1, is chosen as the test fluid and the static contact angle between absolute alcohol and plexiglass is 0° .

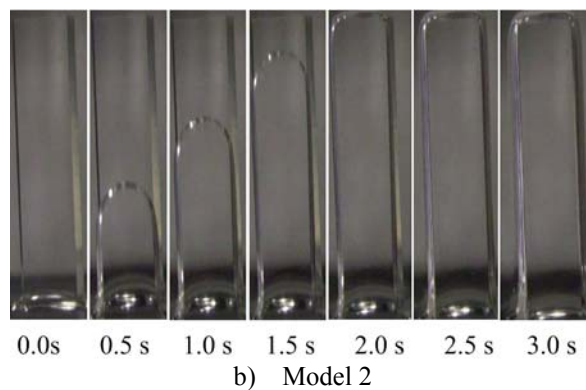
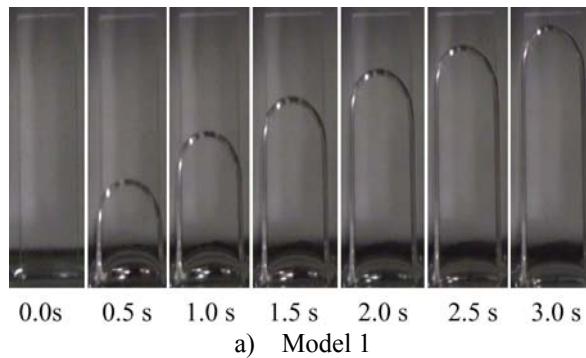
Table 1 Physical properties of absolute alcohol (C_2H_5OH , $20^\circ C$)

Property	Symbol	Unit	Value
surface tension	$\sigma \times 10^{-4}$	N/m	22.03
molecular viscosity	$\mu \times 10^{-4}$	Pa.s	10.56
fluid density	ρ	kg/m ³	793
refractive index	N_d		1.399
static contact angle	θ	$^\circ$	0

3. Results and Discussion

3.1 Experimental results

Figure 5 shows the results for microgravity drop tower test. For each PAV, there are 7 snapshots corresponding to the fluid transportation height along the vane at 0s, 0.5s, 1.0s, 1.5s, 2.0s, 2.5s, and 3.0s. In the figures, horizontal lines are drawn to mark the height of the curved liquid surface's apex in every individual instant. It is obvious that the section of PAV affects the fluid transportation performance.



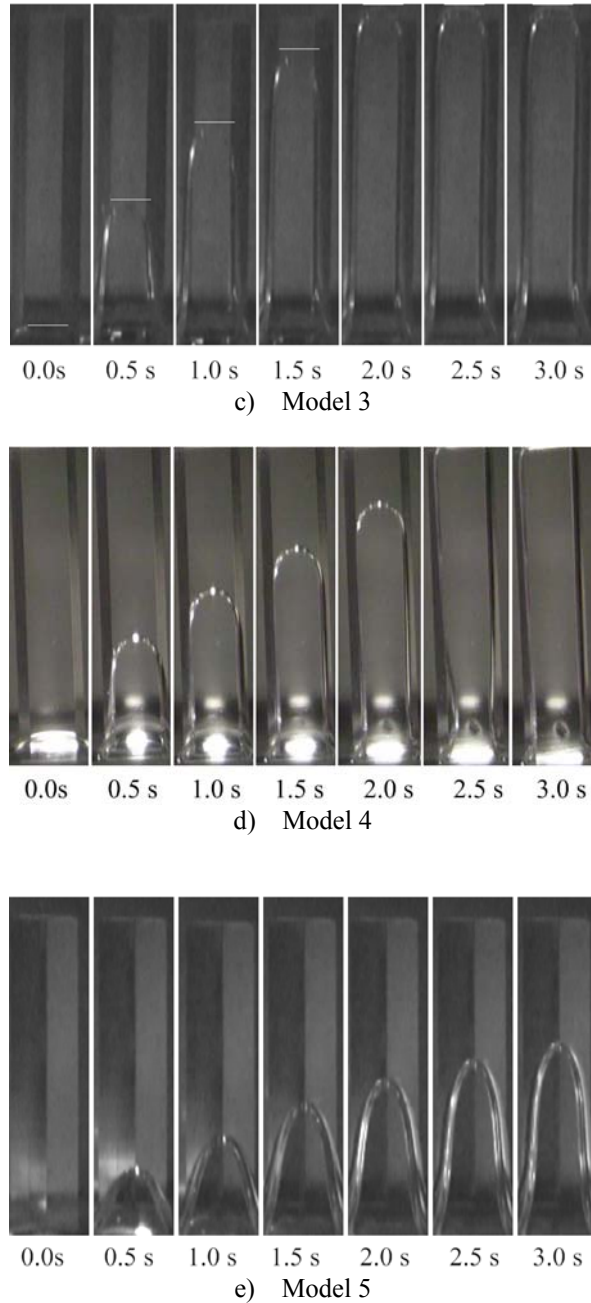


Fig. 5 Fluid transportation performance for 5 PAVs.

At the start of the test process i.e. $t=0s$, each fluid surface is between a PAV and sump wall, and has the convex shape with large curvature radius. The reason is that both surface tension and gravity act together on the fluid. Once the test cabin is released, the acceleration of gravity suddenly reduces to $10^{-5}g$. At the instants, the surface tension plays a dominant role for the fluid movement. Driven by the surface tension, fluid climbs along the surface of a PAV, and the curvature radius of gas-liquid interface is smaller than that at the start. It can be visually seen from pictures that the fluid transportation velocity of different models are quite different. The velocities for Model 2 and Model 3 are faster, and that for Model 5 is the slowest. The height of the curved liquid surface's apex at every interval of 0.04s is measured to obtain the fluid transportation performance for each PAV.

3.2 Numerical calculation results

For numerical simulation, the solver of commercial code Fluent is used. The pressure in equations is treated by Body Force Weighted algorithm and the momentum by QUICK algorithm. A Geo-Construct method is used to discretize the calculation domain. And the PISO algorithm is employed to decouple the velocity and pressure.

Wall boundary condition for every surface is set as no-slip condition, and wall contact angle is set to be constant, 0. Gas and liquid are helium and absolute alcohol. VOF model of multiphase is employed for unsteady calculation. Every time step is 0.002s. In Figure 6, calculation results of liquid transportation for Model 1 is shown.

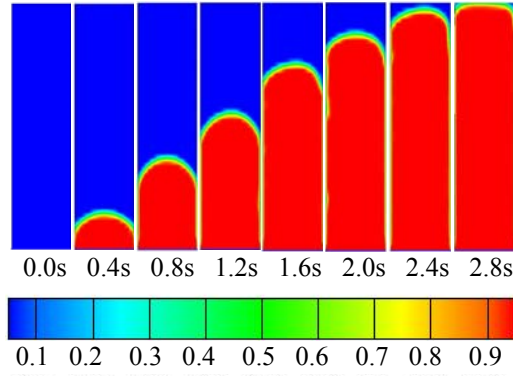


Fig. 6 Calculation results of fluid transportation for Model 1.

Based on numerical results, it takes 2.8s for fluid to climb to the top of the PAV i.e. Model 1. From 0.4s to 2.8s, the propellant climbs up along propellant acquisition vanes, and gas-liquid interface bends to gas side because the surface tension of liquid plays a leading role. Compared with the experimental result, the development of two phase flow along the PAV was predicted fairly well by the present calculation. However, the flow velocity is somehow over-estimated. The possible reason may be the difference for wall roughness and wall contact angle between the numerical calculation and the experiment.

3.3 Discussions

In order to make clear the fluid transportation capability of PAVs in microgravity environment, the relation of gas-liquid interface height with time t , and that with $t^{1/2}$ for different models is shown in Figure 7 and Figure 8. Note that t_0 means the total duration for fluid transportation process.

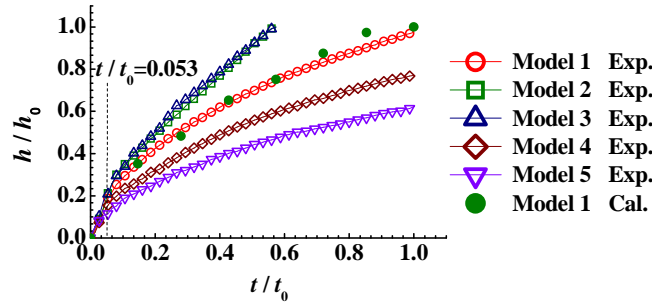


Fig. 7 Relation of gas-liquid interface height with time for different models.

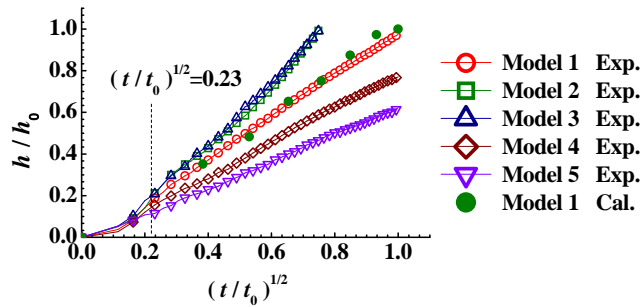


Fig. 8 Relation of gas-liquid interface height with $t^{1/2}$ for different models.

Based on those data, the following can be seen:

1) In microgravity environment, the process of fluid climbing along a PAV can be divided into two stages by the dotted line in Figs. 7 and 8: the relocation period of the liquid-gas interface after gravity disappears, and the steady transportation stage when the surface tension plays a leading role.

For the first stage, the relative time is $0 < t/t_0 < 0.053$ in Figure 7. During the first stage, inertia force of the liquid is dominant and the liquid transports fast. At the same time, gas-liquid interface changes obviously and the biggest relative height for fluid transportation is 0.21.

In Figure 8, the critical time between two stages is $(t/t_0)^{1/2} = 0.23$.

As the effect of microgravity appears, liquid transportation speed decreases because the effect of inertia decreases and that of the viscous force increases. At the second stage, the two phase interface increases steadily.

The transportation velocities for 5 PAV models are much different. There is good linear correlation between relative time's square root $(t/t_0)^{1/2}$ and relative height h/h_0 . That means, in microgravity environment, the propellant transportation height of PAV is proportional to the time's square root $t^{1/2}$. Those results agree to that obtained by Weisloger etc. [14-15], who studied the capillary driven flow in a circular tube experimentally.

2) Section shape of a PAV influences the liquid transportation velocity obviously in microgravity environment.

It is seen that Model 2 and Model 3 have almost the same propellant acquisition capability, and their fluid transportation velocities are the largest. And the fluid transportation velocity of Model 5 is the lowest. Thus, the liquid transportation velocity is affected by the bottom length ratio of PAV such as a_1/a_0 , a_2/a_0 , a_3/a_0 , a_4/a_0 , a_5/a_0 . When the ratios are 1/2 and 5/6, the velocity is the largest. The velocity decreases when the ratio is from 1/3 to 0. For Model 5 where the ratio is 0, the relative height of the interface during 3 seconds is just 0.62. The vane section such as triangle geometry is unsuitable for PAV, especially for devices with only guide vanes.

Those results indicate an effective interface control method in microgravity environment. In general, optimizing the section shapes of a PAV provides a new useful method for controlling fluid in space engineering.

4. Conclusions

The present paper treats fluid transportation behaviors of propellant acquisition vanes (PAVs) with different section geometry by microgravity drop tower test. Based on the results, the following conclusions can be drawn:

1) The section geometry of PAVs is one of the main factors affecting the propellant transportation performance of a vane type PMD. PAVs with bottom length ratio of 5/6 and 1/2 have large propellant transportation velocity.

2) The process of propellant transportation under microgravity environment can be divided into two stages: fluid relocation and steady transportation stage. There is good linear correlation between liquid transportation velocity and relative time's square root.

Acknowledgements

This work was supported by the National Natural Science Foundation of China (Grant No. 51179091), Tsinghua-Yuyuan Medical Fund and the Ministry of Science and Technology of China (Grant No. 2008KR0441).

Nomenclature

a_0	length for the PAVs	h_0	height for the PAVs
b_0	width for the PAVs	t	microgravity time
d	distance to sump surface	t_0	total microgravity time
g	ground gravitational acceleration	ρ	fluid density

References

- [1] J. Tegart, N.T. Wright, 1983, "Double perforated plate as a capillary barrier," AIAA-83-1379.
- [2] M. K. Reagan, W. J. Bowman, 1987, "Analytical and experimental modeling of zero/low gravity fluid behavior," AIAA87-1865.
- [3] D. E. Jaekle, 1991, "Propellant management device conceptual design and analysis: vane," AIAA-91-2172.
- [4] M. K. Reagan, W. J. Bowman, 1999, "Transient studies of G-induced capillary flow," Journal of Thermophysics and Heat Transfer, Vol. 13, No. 4, pp. 537-543.
- [5] M. Strange, G. Wolk, M. Dreyer, et al., 2000, "Drop tower tests on capillary flow in open vanes under lateral acceleration," AIAA 2000-3443.
- [6] D. Lazzer, A. Stange, M. Dreyer, et al., 2003, "Influence of lateral acceleration on capillary interfaces between parallel plates," Microgravity Science and Technology, Vol. 14, No. 4, pp. 3-20.
- [7] D. E. Jaekle, 1995, "Design & development of a communications satellite propellant tank," AIAA-95-2529.
- [8] H. S. Collicott, 2001, "Convergence behavior of Surface Evolver applied to a generic propellant-management device," Journal of Propulsion and Power, Vol. 17, No. 4, pp. 845-851.
- [9] M. M. Weislogel, 2001, "Capillary flow in interior corners: The infinite column," Physics of Fluids, Vol. 13, No. 11, pp. 3101-3107.
- [10] H. S. Collicott, 2000, "Initial experiments on reduced-weight propellant management vanes," AIAA-2000-3442.
- [11] Y. Chen, M. M. Weislogel, C. L. Nardin, 2006, "Capillary-driven flows along rounded interior corners," Journal of Fluid Mechanics, Vol. 56, No. 6, pp. 235-271.
- [12] R. HOU, L. DUAN, L. HU, et al., 2008, "Capillary-driven flows along rounded interior corners in microgravity," Journal of Experiments in Fluid Mechanics, Vol. 22, No. 2, pp. 74-78.
- [13] X. Q. Zhang, L. G. Yuan, W. D. Wu, et al., 2005, "Key technologies of hectometer drop tower test facility of national microgravity laboratory," SCIENCE IN CHINA Ser. E Engineering & Materials Science, Vol. 35, No. 5, pp. 523-534.
- [14] J. N. Burguete, F. Daviaud, N. Carnier, et al., 2001, "Buoyant-thermocapillary instabilities in extended liquid layers subjected to a horizontal temperature gradient," Physics of Fluids, Vol. 13, No. 10, pp. 2773-2787.
- [15] V. M. Shevtsova, A. A. Nepomnyashchy, J. C. Legros, 2003, "Thermocapillary-buoyancy convection in a shallow cavity heated from the side," Physical Review E, Vol. 67, No. 6, pp. 1-14.